



# Opposing spatial trends in methylmercury and total mercury along a peatland chronosequence trophic gradient

Baolin Wang<sup>a</sup>, Mats B. Nilsson<sup>b</sup>, Karin Eklöf<sup>a</sup>, Haiyan Hu<sup>c,d,\*</sup>, Betty Ehnvall<sup>b</sup>, Andrea G. Bravo<sup>e</sup>, Shunqing Zhong<sup>f</sup>, Staffan Åkeblom<sup>a</sup>, Erik Björn<sup>g</sup>, Stefan Bertilsson<sup>a,d</sup>, Ulf Skjällberg<sup>b</sup>, Kevin Bishop<sup>a</sup>

<sup>a</sup> Department of Aquatic Sciences and Assessment, Swedish University of Agricultural Sciences, SE-75007 Uppsala, Sweden

<sup>b</sup> Department of Forest Ecology and Management, Swedish University of Agricultural Sciences, SE-90183 Umeå, Sweden

<sup>c</sup> State Key Laboratory of Environmental Geochemistry, Institute of Geochemistry, Chinese Academy of Sciences, 550081 Guiyang, China

<sup>d</sup> Department of Ecology and Genetics, Limnology and Science for Life Laboratory, Uppsala University, SE-75236 Uppsala, Sweden

<sup>e</sup> Department of Marine Biology and Oceanography, Institut de Ciències del Mar (ICM-CSIC), Pg Marítim de la Barceloneta 37-49, E08003 Barcelona, Catalunya, Spain

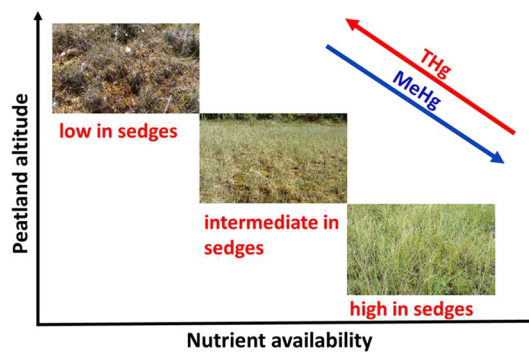
<sup>f</sup> College of City and Tourism, Hengyang Normal University, 421002 Hengyang, China

<sup>g</sup> Department of Chemistry, Umeå University, SE-90187 Umeå, Sweden

## HIGHLIGHTS

- A chronosequence and trophic gradient of peatlands was studied on Hg methylation
- Higher MeHg and %MeHg in younger and more mesotrophic peatlands
- Increasing trophic status positively correlated to the net MeHg production
- Less THg in younger peatlands could indicate more Hg evasion back to the atmosphere

## GRAPHICAL ABSTRACT



## ARTICLE INFO

### Article history:

Received 5 December 2019

Received in revised form 11 February 2020

Accepted 12 February 2020

Available online 13 February 2020

Editor: Mae Sexauer Gustin

### Keywords:

Peatland  
Mercury  
Methylation  
Methylmercury  
Chronosequence

## ABSTRACT

Peatlands are abundant elements of boreal landscapes where inorganic mercury (IHg) can be transformed into bioaccumulating and highly toxic methylmercury (MeHg). We studied fifteen peatlands divided into three age classes (young, intermediate and old) along a geographically constrained chronosequence to determine the role of biogeochemical factors and nutrient availability in controlling the formation of MeHg. In the 10 cm soil layer just below the average annual growing season water table, concentrations of MeHg and %MeHg (of total Hg) were higher in younger, more mesotrophic peatlands than in older, more oligotrophic peatlands. In contrast, total mercury (THg) concentrations were higher in the older peatlands. Partial least squares (PLS) analysis indicates that the net MeHg production was positively correlated to trophic demands of vegetation and an increased availability of potential electron acceptors and donors for Hg methylating microorganisms. An important question for further studies will be to elucidate why there is less THg in the younger peatlands compared to the older peatlands, even though the age of the superficial peat itself is similar for all sites. We hypothesize that ecosystem features which enhance microbial processes involved in Hg methylation also promote Hg reduction that makes previously deposited Hg more available for evasion back to the atmosphere.

© 2020 Elsevier B.V. All rights reserved.

\* Corresponding author at: State Key Laboratory of Environmental Geochemistry, Institute of Geochemistry, Chinese Academy of Sciences, 550081 Guiyang, China.  
E-mail address: [huhaiyan@mail.gyig.ac.cn](mailto:huhaiyan@mail.gyig.ac.cn) (H. Hu).

## 1. Introduction

Methylmercury (MeHg) is a potent neurotoxin, and its bioaccumulation is a pronounced problem in high latitude aquatic ecosystems (AMAP, 2011; Loseto et al., 2004; Macdonald et al., 2005). Biological transformation from inorganic mercury (IHg) to MeHg predominantly occurs in anoxic ecosystems (Benoit et al., 2003; Compeau and Bartha, 1985; Gilmour et al., 2013). Peatlands are known to play an important role in the cycling of Hg in aquatic ecosystems; generally being sinks for total mercury (THg), but net sources of MeHg (Mitchell et al., 2008b; St. Louis et al., 1996; Tjerngren et al., 2012b). MeHg generated in peatlands enters downstream aquatic ecosystems, increasing the risk for harm to humans and wildlife that consume fish from these waters (Driscoll et al., 1994; Munthe et al., 2007; Ratcliffe et al., 1996). The possibilities for mitigating and managing this threat depends on knowing the environmental factors that control the formation of MeHg.

Manipulation experiments have emphasized the dependence of net MeHg formation on the availability of electron acceptors such as sulfate (Åkerblom et al., 2013; Branfireun et al., 2001; Jeremason et al., 2006; Mitchell et al., 2008a), electron donors in the form of high quality carbon exudates from roots (Windham-Myers et al., 2009) and broader climate effects (Bergman et al., 2012). Manipulation experiments, however, are sometimes difficult to generalize to natural environments because of artefacts, such as unintended disturbance effects or the generally limited duration of manipulations. As a complement, field studies along natural gradients have been used to verify experimentally determined factors controlling Hg methylation in peatlands, including sulfate and nutrients. Such studies have generally shown that methylation increases with increasing sulfur and/or nutrient availability to a certain point, beyond which more nutrients and/or sulfur lead to less MeHg (Gilmour et al., 1998; Tjerngren et al., 2012a). In such field studies, though, geographic differences in climate and management history can complicate interpretations of causality.

An ecosystem chronosequence within a restricted geographical area represents a model system that avoids most drawbacks in comparison to more geographically distributed experimental locations. Isostatic rebound since the last glaciation, which continuously raises the coastline around the Gulf of Bothnia between Finland and Sweden at a rate of around 8.2 mm per year (Hünicke et al., 2015), has created chronosequences of boreal ecosystems that can span up to 10,000 years within restricted areas. The major differences between younger and older peatlands across such a chronosequence are increasing peat depth and peatland area with peatland age, together with decreasing delivery of weathering products from the watersheds that deliver dissolved minerals to the older peatlands. All these three factors generate biogeochemical and ecological differences between younger and older peatlands. The biogeochemically active upper decimeters of all the peatlands in the chronosequence, however, have similar ages (several decades). Compared to the surface of the “younger” peatlands, the surface of “older” peatlands on the chronosequence are expected to have lower availability of elements originating from mineral substrates, including all plant nutrients except for nitrogen. This is reflected in significant differences in the plant community composition, with more nutrient demanding vegetation on the younger peatlands (Tuittila et al., 2013). Thus factors which influence the biogeochemistry of significance for mercury biogeochemistry, including potential electron acceptors and donors, as well as plant communities can be expected to vary systematically along a peatland chronosequence. This facilitates studies of long-term biogeochemical influences, and related vegetation changes on the net formation of MeHg without introducing experimental manipulations that would need to be maintained for decades.

In this study, a chronosequence was used to test the hypothesis that net MeHg formation in the surface peat soil along the chronosequence peatlands would change with trophic status as indicated by the availability of minerogenic elements and the quality of organic matter for Hg methylating microorganisms. Those ontogenetic changes would

involve both a decrease in major electron acceptors such as sulfate and Fe(III), as well as a concomitant decrease in electron donors (represented by organic matter quality characteristic of the vegetation composition) with increasing peatland age. These differences would exist despite all of the superficial peat layers sampled along the chronosequence being exposed to a similar climate and atmospheric Hg deposition for a similar period of time. Fifteen peatlands were selected for the study in order to provide sufficient material to resolve the influence of specific environmental factors on Hg cycling and MeHg formation.

## 2. Materials and methods

### 2.1. Site description

Post-glacial land uplift in northern Sweden along the Gulf of Bothnia has created a landscape with many peatlands along an age gradient spanning from 0 to >4000 years within <10 km from the sea. Peatland age since its initiation was obtained according to the shoreline displacement curve for southern Västerbotten that was based on ages dated by the varve-counts of lake sediments and the present-day sea level (Renberg and Segerström, 1981).

The topographic relief of the area is quite low, with small areas of mineral soil up to a meter higher than the peatland. The superficial groundwater tables (ca 10 cm depth on average) have a decimeter of annual variation around the mean. The low topographic relief and the groundwater levels are indicative of a superficial flow system with little regional influences. In this landscape, regional land uplift from the sea creates the conditions for peat to form on what used to be the seabed. Then the growth of that peat successively separates the superficial peat from the underlying sources of minerogenic elements, with lateral minerogenic inputs only from the local “uplands”. The degree of this input is reflected in the unique catchment to peatland ratio (Table S1, Fig. S1 in the Supplementary information (SI)).

An initial vegetation survey of seventy peatlands along the chronosequence was conducted by performing an agglomerative hierarchical clustering of vegetation data (e.g. species and relative species abundance), in which Ward's linkage method and Euclidean distance were used as a group linkage method and a distance measure, respectively. Six vegetation classes (1–6) were clearly clustered, with the increasing number value representing more nutrient demanding vegetation composition (Table 1). Fifteen open peatlands were then selected from three age classes, young (<10 m.a.s.l., <1000 years,  $n = 5$ ), intermediate (10–20 m.a.s.l., 1000–2000 years,  $n = 5$ ) and old (20–40 m.a.s.l., >2000 years,  $n = 5$ ) (Fig. 1). The three peatland age classes were clearly different with respect to elevation, soil acidity (pore water pH), and vegetation composition (Tables 1, S2).

### 2.2. Sampling and sample preparation

Four sampling campaigns were carried out in June (the beginning of the growing season) and August (growing season) of 2016 and 2017. In June 2016, five 70 × 70 cm plots were established within each of the fifteen peatlands. The five plots within each peatland were located at least 5 m away from each other along a line across the center of the peatland. A cube-shaped core of peat soil (10 × 10 × 10 cm) was extracted from each plot of each peatland with a long (60 cm), sharp, custom-made knife. The top of the peat core was defined by the level of the average growing season ground water table (GWT) from the peat soil surface of each peatland. The average GWT ranged from 8.7 cm depth below the soil surface in the young peatlands, to 9.4 cm depth in the intermediate peatlands, and 13.6 cm depth for old peatlands, respectively (Fig. S2). The sampled peat core was cut into upper and lower layers (0–5 and 5–10 cm, respectively). These samples were then sealed in separate plastic zip-lock bags after the air was squeezed out. All the samples were kept in a dark cooling box during transport and stored

**Table 1**  
Characteristics of the study peatlands along the chronosequence.

Peatland	Elevation (m.a.s.l)	Peat depth (cm)	Age (year)	N	E	Veg. class <sup>a</sup>	pH <sup>b</sup>	Temp sum (°C) <sup>c</sup>		Precip (mm) <sup>d</sup>	
								2016	2017	2016	2017
02	0.72	70	72	63°51'3.90"	20°42'54.12"	6	5.0 ± 0.2	1308	1227	230	172
70	1.49	46	149	63°51'8.86"	20°42'35.14"	5	4.0 ± 0.2	1308	1227	230	172
43	3.43	70	341	63°52'11.67"	20°45'8.07"	3	4.0 ± 0.1	1307	1227	232	170
13	3.53	154	352	63°48'38.55"	20°34'51.54"	6	4.5 ± 0.1	1309	1228	223	170
10	5.07	140	503	63°49'9.09"	20°34'41.77"	6	4.1 ± 0.3	1309	1228	223	170
Y <sup>e</sup>	2.8 ± 1.6	98 ± 45	283 ± 154				4.3 ± 0.5	1308	1228	228	171
52	12.60	114	1221	63°57'16.73"	20°46'15.09"	4	4.7 ± 0.2	1300	1221	240	176
14	13.89	244	1341	63°50'54.39"	20°38'39.93"	3	4.5 ± 0.1	1302	1221	229	176
18	14.54	66	1401	63°53'8.15"	20°43'48.29"	4	3.6 ± 0.1	1298	1218	234	176
16	14.56	76	1402	63°52'47.97"	20°42'22.49"	2	3.9 ± 0.3	1298	1218	234	176
62	15.57	106	1495	63°50'37.38"	20°38'16.74"	1	3.8 ± 0.2	1302	1221	229	176
I <sup>f</sup>	14.2 ± 1.0	121 ± 72	1372 ± 90				4.1 ± 0.5	1300	1220	233	176
29	27.53	96	2547	63°52'52.61"	20°38'5.52"	1	3.7 ± 0.2	1296	1215	234	180
26	29.19	246	2686	63°52'5.08"	20°30'28.78"	1	3.7 ± 0.2	1303	1221	229	180
33	30.54	210	2799	63°54'17.68"	20°41'16.43"	2	3.9 ± 0.2	1298	1218	234	176
24	31.46	140	2874	63°51'31.51"	20°29'29.14"	1	3.8 ± 0.2	1303	1221	229	180
65	34.82	130	3146	63°52'58.48"	20°38'50.03"	1	3.8 ± 0.2	1296	1215	234	180
O <sup>g</sup>	30.7 ± 2.4	164 ± 61	2810 ± 200				3.8 ± 0.2	1299	1218	232	179

<sup>c, d</sup> Temperature and precipitation data is from [www.smhi.se](http://www.smhi.se)

<sup>a</sup> Vegetation classes, from an initial survey of seventy peatlands along the chronosequence (data unpublished), with increasing number representing vegetation that requires more nutrients to thrive and spread.

<sup>b</sup> Mean pH ± SD of the four sampling occasions in 2016 and 2017.

<sup>c</sup> Sum of air temperatures during June, July and August in 2016 or 2017.

<sup>d</sup> Sum of precipitation during June, July and August in 2016 or 2017.

<sup>e</sup> Rows represent average parameter values ± SD for young peatland classes.

<sup>f</sup> Rows represent average parameter values ± SD for intermediate peatland classes.

<sup>g</sup> Rows represent average parameter values ± SD for old peatland classes.

in a refrigerator at 4 °C for up to two weeks until further sample preparation. In 2016, the pH was determined in the porewater that immediately refilled the sample hole. While in 2017, the pH was determined in the porewater of the 10 cm peat core that was sampled with a 70 cm long, custom-made, Teflon sampler (Bergman et al., 2012).

All the five upper layers (0–5 cm) taken in the same peatland were homogenized in fresh state through a 4 mm cutting sieve and merged to one composite sample. The homogenization was done after removal of bulky roots, sticks and living plant material. The same was then done for the lower layers (5–10 cm). Immediately after homogenization, approximately 50 g of fresh peat soil was taken and frozen for subsequent determination of MeHg concentration. Triplicate subsamples were taken for the determination of water content by heating at 105 °C until constant mass was achieved. Another ~200 g of subsample was dried at 40 °C until the peat mass was constant. The low temperature was selected to avoid losses of elemental mercury (Hg(0)) (Kodamatani et al., 2017). Dried peat subsamples were used for analysis of concentrations of THg and other elements (e.g. C, N, S) after ball milling (vibrated at 30 Hz for 5 min, Retsch MM400, Retsch GmbH, Germany).

### 2.3. Chemical analyses

The THg in the peat soil dried at 40 °C was analyzed by solid combustion atomic absorption spectrometry (DMA-80, Milestone, Italy) using certified marine sediment reference material MESS-3 (National Research Council of Canada, 0.091 ± 0.009 mg Hg kg<sup>-1</sup>) for calibration. The MeHg content in fresh peatland soils was determined by isotope dilution analysis described in detail elsewhere (Lambertsson et al., 2001; Tjerngren et al., 2012a). Concentration of IHg was calculated by subtracting MeHg from THg. The percentage of MeHg to THg (%MeHg) in the solid peat was also calculated. While the MeHg level itself is of interest for what is transferred from peatlands into downstream ecosystems, the %MeHg in the peat is a better indicator of the net methylation potential (Drott et al., 2008).

Total concentrations of C and N were analyzed on an Elemental analyzer (Flash EA 2000, Thermo Fisher Scientific, Bremen, Germany). Total concentrations of Ca, Fe, Mg, Mn, Na, K, Al, Zn, Si, S and P were determined by ICP-OES (Spectro Ciros Vision, Spectro Analytical Instruments Inc., Germany). These parameters measured by ICP-OES and Elemental analyzer were only measured on the two sampling occasions in 2016,

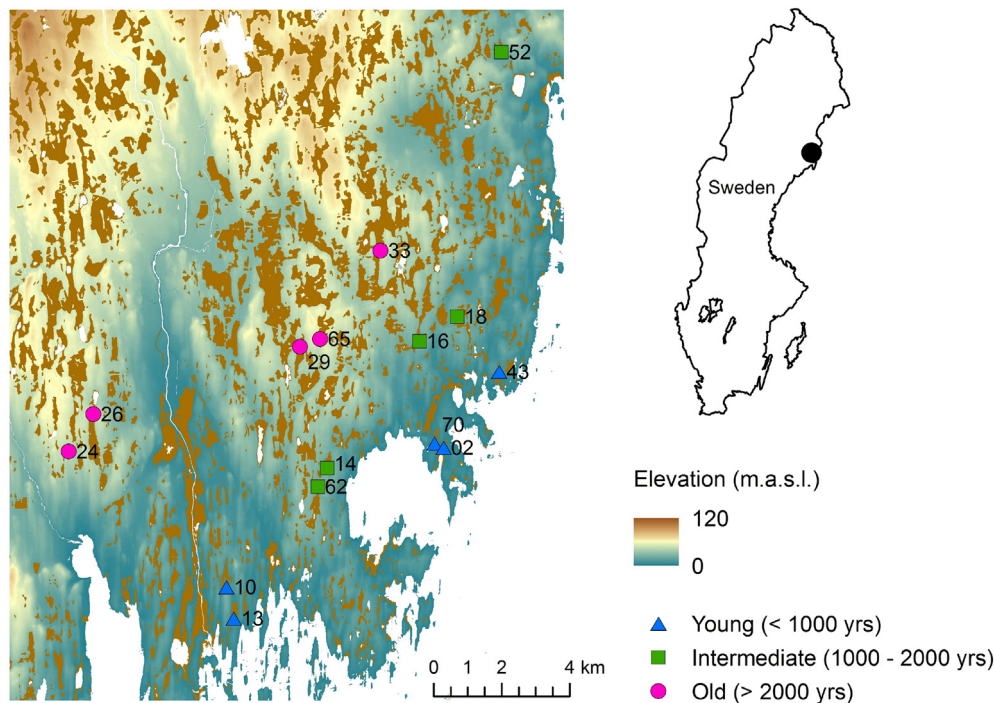


**Fig. 1.** The peatland sampling sites located on the northeast coast of Sweden where post-glacial uplift has created a relationship between elevation above sea level and the age of the peatland. The color of the symbol marking each sampling site indicates the age class (blue triangles = young, green boxes = intermediate, and pink dots = old) assigned to the peatland in this study. The numbering relates to an initial vegetation inventory of some seventy peatlands along this chronosequence. (For interpretation of the references to color in this figure legend, the reader is referred to the web version of this article.)

but not in 2017 as we assumed that the values did not change between 2016 and 2017. Replicate samples and reference material were analyzed regularly and the precision was under 10% relative standard deviation.

#### 2.4. Topographical data

A  $2 \times 2$  m national gridded digital elevation model (DEM) was used to extract hydrological and geomorphological features of the peatlands and their contributing catchments. The high-resolution DEM was generated by the Swedish Mapping, Cadastral and Land Registration Authority (Lantmäteriet) from a LiDAR point cloud with a point density of  $0.5\text{--}1$  points  $\text{m}^{-2}$ , a vertical resolution of 0.3 m and a horizontal resolution of 0.1 m. The DEM was preprocessed prior to the hydrological modelling by burning stream-road intersections and breaching depressions. Flow direction and accumulation were calculated using the deterministic eight-direction flow model (D8) (O'Callaghan and Mark, 1984). All hydrological modelling was performed in Whitebox Geospatial Analysis Tools. The morphological modelling was based on the original DEM and performed in SAGA GIS 6.2.0. Topographic indices used to describe the peatlands and their catchments are documented in Table S1.

#### 2.5. Statistical data analysis

Normality and homogeneity of the data were checked using the Shapiro-Wilkinson test prior to statistical analyses. Log transformation was used to meet the parametric test for normality when the original data were not normally distributed. All the parametric significant differences (e.g. THg, MeHg and %MeHg) across the fifteen peatlands on the four sampling occasions at the two sampling depth (0–5 cm and 5–10 cm below the GWT) were tested by three-way ANOVA, followed by Tukey's multiple comparison test. The three factors tested were peatland type (three age classes), sampling depth (two layers) and month of sampling (June and August). All these tests were carried out at the 0.05 significance level using R (Version 3.6.0). All the statistical analyses involving element concentrations (e.g. total C, N, S) from the

ICP-OES were carried out with the average values of the two 5 cm layers for each peatland on each of the two sampling occasions in 2016. Principle Component Analysis (PCA) and Partial Least Square (PLS) analysis, on non-GIS data, were conducted in the SIMCA software package (Version 14, Umetrics Umeå, Sweden), using only data from the two sampling occasions in 2016. The PCA of GIS derived landscape characteristics, along with %MeHg (average of both 5 cm layers from all the four samplings between 2016 and 2017 on each peatland), were conducted using R (Version 3.6.0).

### 3. Results

#### 3.1. Characteristics of the chronosequence of peatlands

The three age classes along the chronosequence exhibited clear distinctions in vegetation composition and several other geochemical and geomorphological features of the study peatlands that related to the trophic status (Tables S2 and S3). These differences and relationships are evident from the principle component analysis (PCA) (the first two components,  $R^2X = 60\%$ ,  $Q^2 = 40\%$ ). The first principle component (PC1, 43% of total variance) separated old peatlands (positive scores on PC1) from young peatlands (negative scores on PC1), with intermediate peatlands having either positive or negative scores on PC1 (Fig. 2a). The old peatlands, situated at higher elevations above sea level, were slightly more acidic (average porewater pH  $3.8 \pm 0.2$ ; Table S3) and nutrient poor (oligotrophic) than the younger peatlands, as characterized by short growing sedges (*Eriophorum vaginatum*, *Trichophorum* spp. and *Carex limosa*), dwarf shrubs (*Andromeda polifolia* and *Vaccinium oxycoccus*) and *Sphagnum majus*, *Sphagnum balticum* and *Sphagnum papillosum*, in the field- and bottom-layer, respectively (Table S2). The old peatlands had lower concentrations of most minerogenic elements (e.g. Mg, Mn, Fe, K, Na) (negative loadings on PC1) relative to the young and intermediate peatlands (Fig. 2b). The lower minerogenic influence on the old peatlands was also reflected in higher concentrations of C in the superficial peat soil (Table S3) and greater peat depth (Table 1). In contrast,

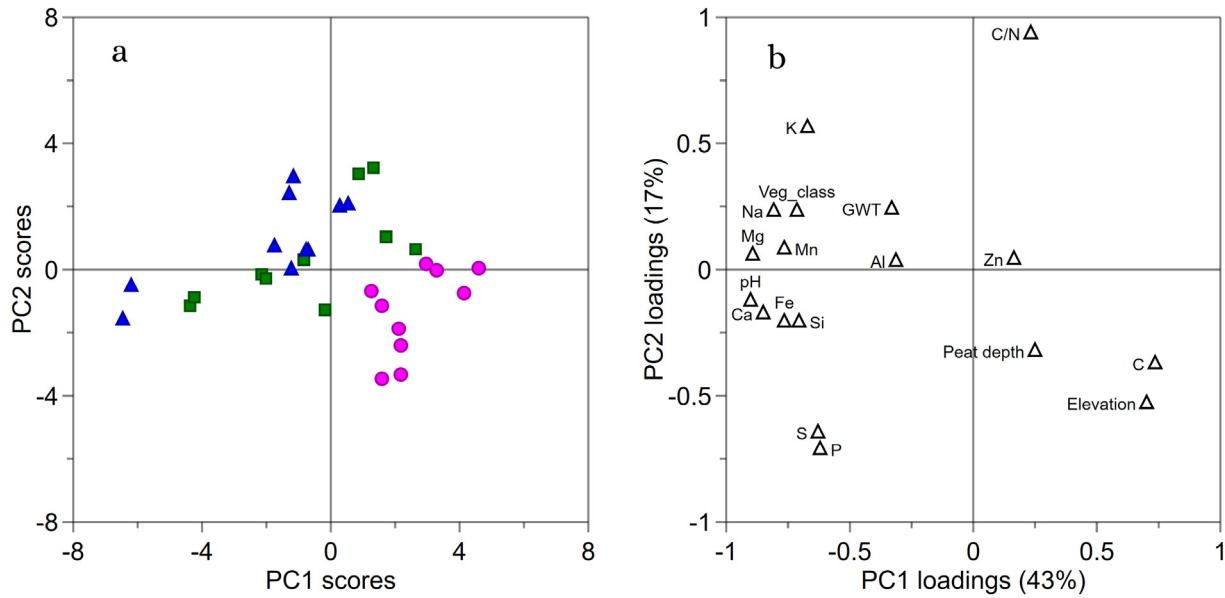


**Fig. 2.** PCA of the explanatory variables (biogeochemistry and vegetation) measured on two sampling occasions during 2016 along a chronosequence of fifteen peatlands. (a) Scores for the three age classes of peatlands, young (blue triangles), intermediate (green boxes) and old (pink dots); (b) Variables strongly contributing to separate the old and young peatland classes have high or low loading respectively for PC1, reflecting the gradient of nutrients and related factors created by peatland aging. It should be noted though, that by sampling the peat immediately below the water table, the age of the peat layer sampled at all sites was similar. Whether the peatland was established 200 years ago or 2000 years ago, the peat material just below the water table is decades old. It is separation from the mineral substrate that increases with age as well as decreasing weathering in any surrounding catchment that differs between the age classes. (For interpretation of the references to color in this figure legend, the reader is referred to the web version of this article.)

young peatlands were less nutrient poor, i.e. mesotrophic, with relatively higher porewater pH ( $4.3 \pm 0.5$ ) and higher minerogenic element concentrations and vegetation classes that require more nutrients to thrive and spread (Fig. 2b and Table S3). The vegetation is characterized by *Carex rostrata*, *Eriophorum vaginatum* and some herbs (e.g. *Potentilla palustris*) in the field layer and *Sphagnum squarrosum*, *Sphagnum fallax* and *Sphagnum riparium* in the bottom layer (Table S2). The intermediate peatlands were intermediate with regards to trophic status, biogeochemistry and vegetation composition.

The younger peatlands were separated from old and intermediate peatlands with regards to hydrological and geomorphological properties (Fig. S1). Peatland and catchment morphological properties (i.e. topographic wetness index (TWI), Elevation above stream (EAS), downslope index (DI), catchment slope, peatland curvature) were some of the features separating young peatlands from old peatlands along the first principal component (29.4% of total variance).

### 3.2. Overall effects on THg, MeHg and %MeHg

The three-way ANOVA models, considering peatland type (three age classes), sampling depth (0–5 and 5–10 cm layers) and month (June and August) explained 37%, 21% and 38% of the variance for THg, MeHg and %MeHg respectively (Table 2). The variations in concentrations of THg, MeHg and %MeHg were significantly explained by peatland age class. The variations in THg and MeHg were also explained by peat layer depth. None of the interaction terms were significant.

### 3.3. Concentrations of THg in peat soil

The old peatlands had higher THg concentrations on all sampling occasions in 2016 and 2017 (average THg of 0–5 and 5–10 cm layers,  $77.2 \pm 26.4$  ng/g dw,  $p < 0.05$ , Tukey's multiple comparison test) compared to young ( $43.6 \pm 15.8$  ng/g) and intermediate peatlands ( $57.5 \pm 24.1$  ng/g). Young and intermediate peatlands were not significantly different in this regard (Fig. 3a and Table S3).

The PLS model of the spatial and temporal variation in THg from the two sampling occasions in 2016 could, with the first two principle components ( $R^2X = 58\%$ ) together, explain 85% ( $R^2Y$ ) and predict 80% ( $Q^2$ )

of the variation in THg across the chronosequence of the fifteen peatlands (Fig. S3a). Variable importance for the projection (VIP) plots

**Table 2**

Three-way ANOVA table for natural log transformed THg, MeHg and %MeHg of the 10 cm peat profile (divided into two 5 cm layers) immediately below the average growing season ground water table in the three peatland age classes along a chronosequence of fifteen peatlands. Boldface “Pr(> F)” indicates significance at  $\alpha = 0.05$ .

Source of variation	Df	Sum Sq	Mean Sq	F value	Pr(>F)	
THg	Peatland age class <sup>a</sup>	2	7.60	3.802	24.53	<b>&lt;0.001</b>
	Month <sup>b</sup>	1	0.001	0.001	0.01	0.935
	Layer <sup>c</sup>	1	1.83	1.83	11.82	<b>&lt;0.001</b>
	Peatland age class × month	2	0.21	0.11	0.68	0.507
	Peatland age class × layer	2	0.21	0.11	0.68	0.508
	Month × layer	1	0.004	0.004	0.02	0.877
	Peatland age class × month × layer	2	0	0	0	0.999
	Residuals	108	16.74	0.155		
	R squared = 0.37					
	MeHg	Peatland age class	2	4.50	2.25	6.92
Month		1	1.19	1.20	3.67	0.058
Layer		1	3.26	3.26	10.01	<b>0.002</b>
Peatland age class × month		2	0.20	0.10	0.30	0.742
Peatland age class × layer		2	0.24	0.12	0.36	0.696
Month × layer		1	0.02	0.02	0.07	0.793
Peatland age class × month × layer		2	0.10	0.05	0.15	0.859
Residuals		108	35.13	0.33		
R squared = 0.21						
%MeHg		Peatland type	2	23.62	11.81	31.34
	Month	1	1.13	1.13	3.00	0.086
	Layer	1	0.20	0.20	0.54	0.464
	Peatland age class × month	2	0.28	0.14	0.38	0.687
	Peatland age class × layer	2	0.12	0.06	0.16	0.857
	Month × layer	1	0.01	0.01	0.02	0.883
	Peatland age class × month × layer	2	0.10	0.05	0.14	0.872
	Residuals	108	40.69	0.38		
	R squared = 0.38					

<sup>a</sup> Peatland age class = young, intermediate and old peatlands.

<sup>b</sup> Sampling occasions in June and August between 2016 and 2017.

<sup>c</sup> Two layers (0–5 and 5–10 cm).

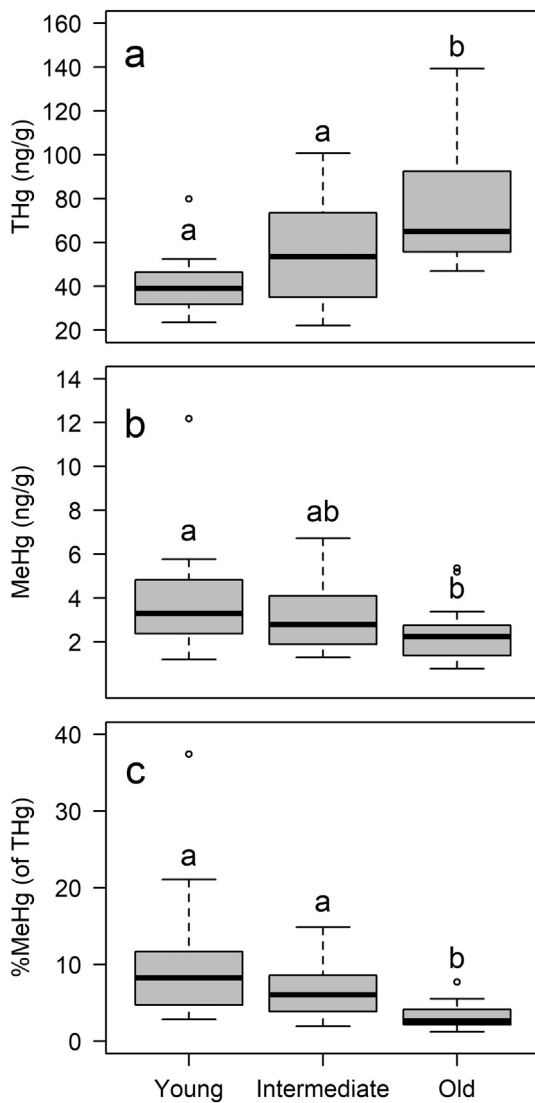


**Fig. 3.** THg (a), MeHg (b) and %MeHg (c) of the 10 cm peat samples collected on four sampling occasions (June and August 2016–2017) along a chronosequence of fifteen peatlands, divided into three age classes, with the average values from both the 0–5 and 5–10 cm layers ( $n = 20$  for each age class). The samples were from 0 to 10 cm below the average growing season ground water table. Thus even though the total age of the peatlands varied as indicated by the age classes, the absolute age of the peat in all these samples was on the order of decades. The “age” indicates the amount time since the peat was established, during which time peat growth has separated the superficial peat from the mineral substrate. Letters above boxes indicate significant differences ( $p < 0.05$ ) between the three age classes, classes with the same letter do not differ significantly.

summarize the importance of the explanatory variables (X) for the response variable(s) (Y), with VIP-values larger than one indicating “important” X-variables. The important variables of the PLS model for THg were K, C/N, elevation, S, C, Mg, Al, and vegetation class (Fig. 4a). The explanatory variables having a significant positive correlation with THg concentrations included those that were characteristic for old peatlands, such as high C concentrations and elevation. In contrast, those that were high in the younger peatlands, such as Mg, Mn, Ca, Na, pH and more nutrient demanding vegetation classes characterized by herbs and tall sedges, correlated negatively with THg (Fig. S3a).

### 3.4. Concentrations of MeHg in peat soil

MeHg concentrations were higher in young peatlands (average MeHg of 0–5 and 5–10 cm layers,  $4.0 \pm 3.2$  ng/g dw) than in old

peatlands ( $2.5 \pm 1.6$  ng/g), with no difference between young and intermediate ones ( $3.4 \pm 1.8$  ng/g) or between intermediate and old ones (Fig. 3b, Table S3). While month of sampling was not significant (Table 2), there was more variation in MeHg concentrations in August 2016 (wet summer, higher GWT, precipitation during June and August = 231 mm) compared to August 2017 (dry summer, lower GWT, precipitation during June and August = 175 mm) (Table 1, Figs. S2, S4).

The PLS model with MeHg as dependent variable explained 69% of the variance in MeHg concentrations with the first two PLS-components ( $R^2X = 52\%$ ,  $Q^2 = 38\%$ ; Fig. S3b). The variables with the highest VIP in this model were Zn, GWT, Ca, pH, Fe and Mg (Fig. 4b). The concentration of MeHg was positively correlated to variables high in young peatlands (e.g. pH, Ca, Fe, S, Mg, Mn) and negatively correlated to those characteristic for old peatlands (e.g. high elevation, C and IHg) (Table S3, Fig. S3b). Interestingly, P and Zn, which were not statistically different across the three age classes of peatlands (Table S3), correlated positively and negatively with MeHg respectively (Fig. S3b).

### 3.5. %MeHg in peat soil

Similar to MeHg, %MeHg was higher in young (average %MeHg of 0–5 and 5–10 cm layers,  $10.9 \pm 10.7\%$ ) and intermediate peatlands ( $7.2 \pm 4.8\%$ ) than in old peatlands ( $3.2 \pm 1.9\%$ ), with no difference between young and intermediate peatlands (Fig. 3c, Table S3). While there was no statistical difference in %MeHg between June and August 2017 (Fig. S5), there was more variation in August 2016 compared to August 2017 (Fig. S5).

Using %MeHg as the response variable resulted in a substantially stronger PLS model (the first two components,  $R^2X = 54\%$ ,  $R^2Y = 82\%$ ,

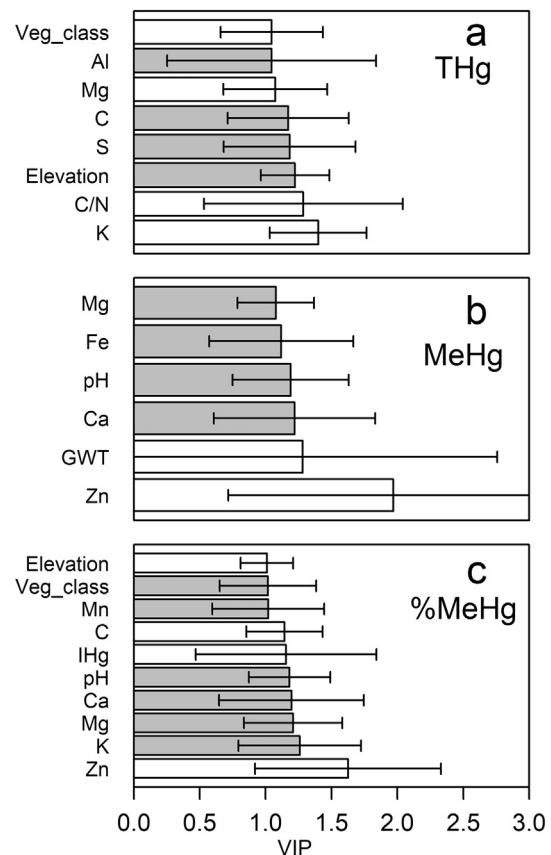


**Fig. 4.** Major explanatory variables of PLS models with THg (a), MeHg (b) and %MeHg (c) as dependent variables. The displayed variables are selected according to variable importance for the projection ( $VIP > 1$ ). Variables displayed with gray bars in each plot correlated positively with corresponding independent variable, while unfilled bars correlated negatively.

$Q^2 = 62\%$ ) than for MeHg. The relatively higher  $Q^2$ -value also indicates a more robust model than for just MeHg (Fig. S3c). The important variables for the projection in this model were Zn, K, Mg, Ca, pH, IHg, C, Mn, vegetation class and elevation (Fig. 4c). The relationship between the explanatory variables and the independent variable here (i.e. % MeHg) was similar to that of the MeHg PLS-model with positive correlations to pH, K, Ca, Fe, Mg, Mn and negative correlations to C and IHg (Fig. S3c). The concentrations of Zn, which were not significantly different along the three age classes (Table S3), correlated strongly and negatively with %MeHg (Fig. S3c).

The PCA of GIS derived landscape characteristics, along with average %MeHg of the two 5 cm layers from all four samplings during 2016–2017 for each peatland, showed that catchment topographic position index 500 (TPI500), peatland DI and EAS correlated negatively with %MeHg, while peatland TWI correlated positively with %MeHg, indicating a hydrological influence on net MeHg production (Fig. S1). Apart from these indices, peatland and catchment elevation as well as age correlated significantly with %MeHg, which was already clear in Fig. 2.

#### 4. Discussion

The peatland chronosequence provides a natural gradient of trophic status and hydrogeochemistry due to the successive isolation of the peat surface from mineral substrates caused by the increasing peat depth, increasing lateral extent of peatland area and decreasing weathering rates in the watershed as peatlands age. This increasing isolation of the vegetation growing each year at the peatland surface explains why increasing peatland age correlated with declining concentrations of minerogenic elements such as Mn, Mg and Fe. These elements are derived primarily from the mineral parent material on which the peat grows, or runoff of weathering products from the surrounding catchment (Fig. 2, Table S3). This decline in minerogenic elements also coincided with a lower pH and declining nutrient availability with age along the chronosequence, as reflected by the change in vegetation composition (Table S2). Along this trophic gradient, both MeHg concentrations and apparent Hg net methylation potential (%MeHg) in the solid peat were higher in the young and mesotrophic peatlands compared to the old and oligotrophic peatlands (Fig. 3, Table S3). This is in agreement with our main hypothesis that MeHg formation will be stimulated in more nutrient-rich peatlands, i.e. mesotrophic peatlands in this study, due to higher nutrient availability to Hg methylating microbes.

The ontogenetic changes in net MeHg formation along this chronosequence of varied trophic status may be due to changes in the activity of Hg methylating microorganisms, including sulfate-reducing bacteria (SRB), iron-reducing bacteria (FeRB), methanogens, syntrophs, and *Firmicutes* (Compeau and Bartha, 1985; Fleming et al., 2006; Gilmour et al., 1992; Gilmour et al., 2013; Hamelin et al., 2011; Kerin et al., 2006; Wood et al., 1968; Yu et al., 2018). Our study focused on the 10 cm of peat soil sampled immediately below the average growing season GWT. This is an area where water table fluctuations create redox oscillations likely to favor microbial processes such as reduction of sulfate and ferric iron, both of which are implicated in Hg methylation (Bergman et al., 2012), and where organic matter degradation, for example by syntrophs (Bae et al., 2014; McInerney et al., 2009; Stams and Plugge, 2009; Yu et al., 2018), offer electrons to Hg methylating microbes. In the young peatlands, higher concentrations of potential electron acceptors such as iron (when oxidized) (Bravo et al., 2018) (Fig. 2 and Table S3) as well as more potential sources of electron donors in labile organic matter of root exudates from vascular sedges (Haynes et al., 2017; Windham-Myers et al., 2009) (Table S2) could stimulate higher methylator activity, leading to the higher MeHg concentration and % MeHg observed in the young peatlands (Fig. 3b, c).

We analyzed the upper and lower halves of this 10 cm layer below the average GWT separately, and the concentrations of both MeHg as well as THg were somewhat greater in the deeper (5–10 cm) layer

compared to the more superficial (0–5 cm) layer. There was, however, no difference in the %MeHg between the two layers (Table 2). Furthermore, there were also no differences in THg, MeHg and %MeHg between the June and August samplings (Table 2, Figs. S4, S5). This suggests that other than the depth differences in MeHg and THg, there were no distinct vertical gradients in the net methylation potential within the decimeter below the annual mean growing season GWT, and that there were no major temporal differences in the studied parameters during the snow-free season.

The finding that Hg net methylation potential (%MeHg) was lower in the more oligotrophic, old peatlands is in agreement with previous research demonstrating that nutrient status influences net MeHg production, with a peak in production at intermediate nutrient availability (Tjerngren et al., 2012b). However, this optimal nutrient level is not surpassed in the chronosequence studied here, as these only cover the lower range (acidic part) of the nutrient gradient (Table S3).

The change in apparent Hg net methylation potential with indicators of wetness, which also correlate with age and trophic status, is reflected in the GIS derived landscape characteristics (Fig. S1, Table S1). The correlations with TWI, DI and EAS of peatlands suggest that Hg methylation is a function of wetness where a higher average peatland wetness (high TWI, low DI, low EAS) leads to a higher methylation potential.

One additional factor that could promote Hg methylation is the presence of a large pool of Hg. There was, however, a negative relationship between %MeHg and IHg across the peatland chronosequence (Table S3, Fig. S3c). Hence higher IHg does not seem to promote Hg methylation in these ecosystems. This result agrees with other studies that have not found bulk Hg as a factor controlling MeHg formation (Åkerblom et al., 2013; Branfireun et al., 2001), leading us to conclude that other factors such as methylator/demethylator activity and the availability of specific Hg species control net MeHg formation.

The difference in THg in the superficial peat along this peatland chronosequence (Fig. 3a) raises the question of a causal mechanism. Even though the peatlands at 20–40 m elevation are thousands of years older than those closer to sea level, the actual age of the peat being sampled just below the GWT is expected to be similar (several decades) for all of the sampled peatlands. Thus the sampled peat material should have been exposed to the same Hg deposition and atmospheric concentrations independent of peatland age. It must therefore be something about the environment of the younger peats that either prevents accumulation of Hg or removes deposited Hg from the surface peat, either back to the atmosphere or to the downstream aquatic ecosystems.

Peat decomposition indicated by bulk density and C/N ratio of peat is suggested to influence Hg retention (Biester et al., 2012; Rydberg et al., 2010), but there was no statistical difference in bulk density or C/N ratio between the three peatland classes (Table S3). This suggests that peat decomposition is not responsible for the differences in Hg concentrations between the three peatland classes along the chronosequence. Vegetation type and composition can also affect both Hg concentration and long-term accumulation in peatlands. It has been reported that open *Sphagnum* fens have lower Hg concentrations and net accumulation than pine-covered fens and that *Sphagnum* mosses sequester more Hg compared to vascular plants (Rydberg et al., 2010). In this study, all sites are open *Sphagnum* areas, so tree cover should not be a factor. The young peatlands have a denser cover of vascular plants compared to old peatlands (Table S2), so this may contribute to less THg in the young peatlands, even though sphagnum is the main vegetation at all sites.

Jiskra et al. (2015) have inferred Hg evasion from organic forest soils within 100 km of our study area based on the isotopic signature of the soils. Furthermore, the first full year measurement of land-atmosphere exchange over a peat bog (further inland from the chronosequence in this study) has demonstrated Hg evasion back to the atmosphere at a rate three times higher than the rate of wet deposition (Osterwalder et al., 2017). This establishes that net Hg(0) evasion is possible, possibly as a response to declines in regional atmospheric Hg(0) concentrations

of 50% since the 1980s (Streets et al., 2011). However, the above-mentioned micrometeorological study was carried out on a single peatland at the old and nutrient poor end of the spectrum included in the current study, and does thus not inform us about how evasion rates may vary with nutrient status.

Advective losses of Hg associated with water moving through and out of peatland ecosystems also occur. However, the precipitation (and presumably runoff) is similar across all the sites (Table 1), so it would need to be concentration differences in the advective flows that could explain the age-related differences. Furthermore, the Hg evasion was also seven times greater than stream Hg export from the peatland where Hg evasion was measured (Osterwalder et al., 2017). If higher THg in old peatlands in this study is a result of less evasion from older peatlands than younger peatlands along the chronosequence during recent decades, then it suggests that the same factors that promote Hg methylation may also promote Hg(0) evasion. In fact, a decade of experimental sulfate addition to a part of that older peatland where the micrometeorological study was conducted (Osterwalder et al., 2017), significantly reduced the THg in the peat (Åkerblom et al., 2013), while at the same time stimulating methylation during much of the growing season (Bergman et al., 2012).

Assuming that all of the observed difference in THg content of young and old peatlands in the peat layer 0–10 cm below the GWT was due to evasion over the past 30 years from only that layer, then the difference in Hg content between the old peatlands (263  $\mu\text{g}/\text{m}^2$ ) and the young peatlands (102  $\mu\text{g}/\text{m}^2$ ) could be explained by 5.4  $\mu\text{g}/\text{m}^2/\text{year}$  more evasion from the younger peatlands, relative to the older peatlands. The evasion from the younger peatlands would be in addition to any evasion from older peatlands. The net Hg evasion rate from an older peatland in the region was 10  $\mu\text{g}/\text{m}^2/\text{year}$  during 2013–2014 (Osterwalder et al., 2017).

Reduction of oxidized Hg(0) was also suggested to be a key factor in the evasion of Hg from that peatland studied by Osterwalder et al. (2017) who observed a temporal correlation between evasion of Hg from the peat surface and the concentration of dissolved gaseous Hg in the peatland porewater just below the water table. If microbial reduction of oxidized Hg were a feature of this environment, this could explain both the evasion of Hg that is reduced to Hg(0) and increased Hg methylation potential (as oxidized IHg is rendered available for methylation) in the younger peatlands. Microbial Hg(0) formation can occur under dark and anaerobic conditions by dissimilatory metal-reducing bacteria (Hu et al., 2013; Wiatrowski et al., 2006), and some of them (e.g. *Geobacter sulfurreducens*) are also known to be capable of methylating Hg (Schaefer and Morel, 2009). The activity of such bacteria could be stimulated by the higher concentrations of electron acceptors such as ferric iron and some other elements observed in the younger peatlands together with more labile root exudates of organic matter expected from the more productive vegetation composition in younger peatlands (Tables S2, S3) (Åkerblom et al., 2013; Windham-Myers et al., 2009; Yu et al., 2012). Furthermore, the incubation experiments in Hu et al. (2020) with samples from three of the peatlands in this study showed that the rates of both Hg methylation and MeHg demethylation were highest in the younger peatland, setting up conditions that might not only fuel the growth of microbes but also make Hg more available for Hg reduction to elemental Hg which is more susceptible to evade back to the atmosphere. This would be consistent with higher re-emission of Hg(0) from young peatlands as well as the promotion of Hg methylation in these systems.

The results from this study contribute to a better understanding of the large scale patterns of Hg accumulation and Hg evasion from peatlands in both space and time, and also inform us about characteristics that are likely to promote Hg methylation and Hg evasion. The inverse relationship between net MeHg production and THg content of peat along the chronosequence of peatlands is striking. These ecosystems have been exposed to similar Hg deposition and climate for centuries, enabling us to map differences in biogeochemical pathways of Hg

cycling as peatland age. We propose that future research on Hg transformations in the boreal landscape could benefit from quantifying the Hg evasion rates along these MeHg formation gradients as well as combining isotopic and genomic approaches for better understanding of the mechanisms behind the interplay between MeHg formation and Hg evasion.

### CRediT authorship contribution statement

**Baolin Wang:** Writing - original draft, Visualization, Investigation. **Mats B. Nilsson:** Writing - review & editing, Methodology, Conceptualization. **Karin Eklöf:** Writing - review & editing. **Haiyan Hu:** Writing - review & editing, Conceptualization. **Betty Ehnvall:** Formal analysis, Visualization, Investigation. **Andrea G. Bravo:** Writing - review & editing. **Shunqing Zhong:** Formal analysis. **Staffan Åkerblom:** Formal analysis. **Erik Björn:** Writing - review & editing, Methodology. **Stefan Bertilsson:** Writing - review & editing, Methodology. **Ulf Skjällberg:** Writing - review & editing, Conceptualization. **Kevin Bishop:** Writing - review & editing, Supervision, Funding acquisition, Conceptualization.

### Declaration of competing interest

The authors declare that they have no known competing financial interests or personal relationships that could have appeared to influence the work reported in this paper.

### Acknowledgments

This work was supported by the China Scholarship Council (CSC, 2015–2018), the Sino-Swedish Mercury Management Research Framework (SMaReF: VR2013-6978), the National Natural Science Foundation of China (No. 41573078 and 41303098) and the Swedish Research Council Formas (2106-00896). Thanks to Tao Jiang, Nguyen Liem, Yu Song and Wei Zhu for their assistance in the laboratory. Thanks to Lucas Perreal, Camille Guyenot, Thibaut Imbert, Edward van Westrene, Marloes Arens, Mélissa Garsany, Laura Manteau, Jeanne Latour, Charles Sanseverino, Quan Zhou and Itziar Aguinaga Gil for the help with the field work.

### Appendix A. Supplementary data

Supporting Information contains 5 Figures and 3 tables, specifically on PCA of the topographic indices, ground water table, PLS analyses for THg, MeHg and %MeHg, as well as differences in MeHg and %MeHg between June and August samplings. Description of morphological and topographical indices, vegetation composition, chemical parameters of peat soil. Supplementary data to this article can be found online at <https://doi.org/10.1016/j.scitotenv.2020.137306>.

### References

- Åkerblom, S., Bishop, K., Björn, E., Lambertsson, L., Eriksson, T., Nilsson, M.B., 2013. Significant interaction effects from sulfate deposition and climate on sulfur concentrations constitute major controls on methylmercury production in peatlands. *Geochim. Cosmochim. Acta* 102, 1–11.
- AMAP, 2011. AMAP Assessment 2011: Mercury in the Arctic. Arctic Monitoring and Assessment Programme (AMAP).
- Bae, H.S., Dierberg, F.E., Ogram, A., 2014. Syntrophs dominate sequences associated with the mercury methylation-related gene *hgcA* in the water conservation areas of the Florida Everglades. *Appl. Environ. Microbiol.* 80, 6517–6526.
- Benoit, J.M., Gilmour, C.C., Heyes, A., Mason, R.P., Miller, C.L., 2003. Geochemical and biological controls over methylmercury production and degradation in aquatic ecosystems. *Biogeochemistry of Environmentally Important Trace Elements*. 835. American Chemical Society, pp. 262–297.
- Bergman, I., Bishop, K., Tu, Q., Frech, W., Åkerblom, S., Nilsson, M., 2012. The influence of sulphate deposition on the seasonal variation of peat pore water methyl Hg in a boreal mire. *PLoS One* 7, 10.
- Bieber, H., Hermanns, Y.-M., Martínez Cortizas, A., 2012. The influence of organic matter decay on the distribution of major and trace elements in ombrotrophic mires – a case study from the Harz Mountains. *Geochim. Cosmochim. Acta* 84, 126–136.



- Branfiren, B.A., Bishop, K., Roulet, N.T., Granberg, G., Nilsson, M., 2001. Mercury cycling in boreal ecosystems: the long-term effect of acid rain constituents on peatland pore water methylmercury concentrations. *Geophys. Res. Lett.* 28, 1227–1230.
- Bravo, A.G., Zopfi, J., Buck, M., Xu, J., Bertilsson, S., Schaefer, J.K., et al., 2018. Geobacteraceae are important members of mercury-methylating microbial communities of sediments impacted by waste water releases. *ISME J.* 12, 802–812.
- Compeau, G.C., Bartha, R., 1985. Sulfate-reducing bacteria: principal methylators of mercury in anoxic estuarine sediment. *Appl. Environ. Microbiol.* 50, 498–502.
- Driscoll, C.T., Yan, C., Schofield, C.L., Munson, R., Holsapple, J., 1994. The mercury cycle and fish in the Adirondack lakes. *Environ. Sci. Technol.* 28, 136A–143A.
- Drott, A., Lambertsson, L., Björn, E., Skjällberg, U., 2008. Do potential methylation rates reflect accumulated methyl mercury in contaminated sediments? *Environ. Sci. Technol.* 42, 153–158.
- Fleming, E.J., Mack, E.E., Green, P.G., Nelson, D.C., 2006. Mercury methylation from unexpected sources: molybdate-inhibited freshwater sediments and an iron-reducing bacterium. *Appl. Environ. Microbiol.* 72, 457–464.
- Gilmour, C.C., Henry, E.A., Mitchell, R., 1992. Sulfate stimulation of mercury methylation in freshwater sediments. *Environ. Sci. Technol.* 26, 2281–2287.
- Gilmour, C.C., Riedel, G.S., Ederington, M.C., Bell, J.T., Gill, G.A., Stordal, M.C., 1998. Methylmercury concentrations and production rates across a trophic gradient in the northern Everglades. *Biogeochemistry* 40, 327–345.
- Gilmour, C.C., Podar, M., Bullock, A.L., Graham, A.M., Brown, S.D., Somenahally, A.C., et al., 2013. Mercury methylation by novel microorganisms from new environments. *Environ. Sci. Technol.* 47, 11810–11820.
- Hamelin, S., Amyot, M., Barkay, T., Wang, Y., Planas, D., 2011. Methanogens: principal methylators of mercury in lake periphyton. *Environ. Sci. Technol.* 45, 7693–7700.
- Haynes, K.M., Kane, E.S., Potvin, L., Lilleskov, E.A., Kolka, R.K., Mitchell, C.P.J., 2017. Mobility and transport of mercury and methylmercury in peat as a function of changes in water table regime and plant functional groups. *Glob. Biogeochem. Cycles* 31, 233–244.
- Hu, H., Lin, H., Zheng, W., Rao, B., Feng, X., Liang, L., et al., 2013. Mercury reduction and cell-surface adsorption by *Geobacter sulfurreducens* PCA. *Environ. Sci. Technol.* 47, 10922–10930.
- Hu, H., Wang, B., Bravo, A.G., Björn, E., Skjällberg, U., Amouroux, D., et al., 2020. Shifts in mercury methylation across a peatland chronosequence: from sulfate reduction to methanogenesis and syntrophy. *J. Hazard. Mater.* 387, 121967.
- Hünicke, B., Zorita, E., Soomere, T., Madsen, K.S., Johansson, M., Suursaar, Ü., 2015. Recent change—sea level and wind waves. In: *BIAT, T. (Ed.), Second Assessment of Climate Change for the Baltic Sea Basin*. Springer International Publishing, Cham, pp. 155–185.
- Jeremiason, J.D., Engstrom, D.R., Swain, E.B., Nater, E.A., Johnson, B.M., Almendinger, J.E., et al., 2006. Sulfate addition increases methylmercury production in an experimental wetland. *Environ. Sci. Technol.* 40, 3800–3806.
- Jiskra, M., Wiederhold, J.G., Skjällberg, U., Kronberg, R.-M., Hajdas, I., Kretzschmar, R., 2015. Mercury deposition and re-emission pathways in boreal forest soils investigated with hg isotope signatures. *Environ. Sci. Technol.* 49, 7188–7196.
- Kerin, E.J., Gilmour, C.C., Roden, E., Suzuki, M.T., Coates, J.D., Mason, R.P., 2006. Mercury methylation by dissimilatory iron-reducing bacteria. *Appl. Environ. Microbiol.* 72, 7919–7921.
- Kodamatani, H., Maeda, C., Balogh, S.J., Nolle, Y.H., Kanzaki, R., Tomiyasu, T., 2017. The influence of sample drying and storage conditions on methylmercury determination in soils and sediments. *Chemosphere* 173, 380–386.
- Lambertsson, L., Lundberg, E., Nilsson, M., Frech, W., 2001. Applications of enriched stable isotope tracers in combination with isotope dilution GC-ICP-MS to study mercury species transformation in sea sediments during in situ ethylation and determination. *J. Anal. At. Spectrom.* 16, 1296–1301.
- Loseto, L.L., Siciliano, S.D., Lean, D.R., 2004. Methylmercury production in high arctic wetlands. *Environ. Toxicol. Chem.* 23, 17–23.
- Macdonald, R.W., Harner, T., Fyfe, J., 2005. Recent climate change in the Arctic and its impact on contaminant pathways and interpretation of temporal trend data. *Sci. Total Environ.* 342, 5–86.
- McInerney, M.J., Sieber, J.R., Gunsalus, R.P., 2009. Syntrophy in anaerobic global carbon cycles. *Curr. Opin. Biotechnol.* 20, 623–632.
- Mitchell, C.P.J., Branfiren, B.A., Kolka, R.K., 2008a. Assessing sulfate and carbon controls on net methylmercury production in peatlands: an in situ mesocosm approach. *Appl. Geochem.* 23, 503–518.
- Mitchell, C.P.J., Branfiren, B.A., Kolka, R.K., 2008b. Spatial characteristics of net methylmercury production hot spots in peatlands. *Environ. Sci. Technol.* 42, 1010–1016.
- Munthe, J., Bodaly, R.A., Branfiren, B.A., Driscoll, C.T., Gilmour, C.C., Harris, R., et al., 2007. Recovery of mercury-contaminated fisheries. *BIOONE* 36.
- O'Callaghan, J.F., Mark, D.M., 1984. The extraction of drainage networks from digital elevation data. *Computer Vision, Graphics, and Image Processing* 28, 323–344.
- Osterwalder, S., Bishop, K., Alewell, C., Fritsche, J., Laudon, H., Åkerblom, S., et al., 2017. Mercury evasion from a boreal peatland shortens the timeline for recovery from legacy pollution. *Sci. Rep.* 7, 16022.
- Ratcliffe, H.E., Swanson, G.M., Fischer, L.J., 1996. Human exposure to mercury: a critical assessment of the evidence of adverse health effects. *J. Toxicol. Environ. Health* 49, 221–270.
- Renberg, I., Segerström, U., 1981. The initial points on a shoreline displacement curve for southern Västerbotten, dated by varve-counts of lake sediments. In: Königsson, L.-K., Paabo, K. (Eds.), *Florilegium Florinis Dedicatum*. 14. Striae, Uppsala, pp. 174–176.
- Rydberg, J., Karlsson, J., Nyman, R., Wanhatalo, I., Nätke, K., Bindler, R., 2010. Importance of vegetation type for mercury sequestration in the northern Swedish mire, Rödmosamyran. *Geochim. Cosmochim. Acta* 74, 7116–7126.
- Schaefer, J.K., Morel, F.M.M., 2009. High methylation rates of mercury bound to cysteine by *Geobacter sulfurreducens*. *Nat. Geosci.* 2, 123–126.
- St. Louis, V.L., JWM, R., Kelly, C.A., Beaty, K.G., Flett, R.J., Roulet, N.T., 1996. Production and loss of methylmercury and loss of total mercury from boreal forest catchments containing different types of wetlands. *Environ. Sci. Technol.* 30, 2719–2729.
- Stams, A.J.M., Plugge, C.M., 2009. Electron transfer in syntrophic communities of anaerobic bacteria and archaea. *Nat. Rev. Microbiol.* 7, 568–577.
- Streets, D.G., Devane, M.K., Lu, Z., Bond, T.C., Sunderland, E.M., Jacob, D.J., 2011. All-time releases of mercury to the atmosphere from human activities. *Environ. Sci. Technol.* 45, 10485–10491.
- Tjerngren, I., Karlsson, T., Björn, E., Skjällberg, U., 2012a. Potential Hg methylation and MeHg demethylation rates related to the nutrient status of different boreal wetlands. *Biogeochemistry* 108, 335–350.
- Tjerngren, I., Meili, M., Björn, E., Skjällberg, U., 2012b. Eight boreal wetlands as sources and sinks for methyl mercury in relation to soil acidity, C/N ratio, and small-scale flooding. *Environ. Sci. Technol.* 46, 8052–8060.
- Tuittila, E.-S., Juutinen, S., Frolking, S., Väiranta, M., Laine, A.M., Miettinen, A., et al., 2013. Wetland chronosequence as a model of peatland development: vegetation succession, peat and carbon accumulation. *The Holocene* 23, 25–35.
- Wiatrowski, H.A., Ward, P.M., Barkay, T., 2006. Novel reduction of mercury(II) by mercury-sensitive dissimilatory metal reducing bacteria. *Environ. Sci. Technol.* 40, 6690–6696.
- Windham-Myers, L., Marvin-Dipasquale, M., Krabbenhoft, D.P., Agee, J.L., Cox, M.H., Heredia-Middleton, P., et al., 2009. Experimental removal of wetland emergent vegetation leads to decreased methylmercury production in surface sediment. *J. Geophys. Res. Biogeosci.* 114.
- Wood, J.M., Kennedy, F.S., Rosen, C.G., 1968. Synthesis of methyl-mercury compounds by extracts of a methanogenic bacterium. *Nature* 220, 173–174.
- Yu, R.-Q., Flanders, J., Mack, E.E., Turner, R., Mirza, M.B., Barkay, T., 2012. Contribution of coexisting sulfate and iron reducing bacteria to methylmercury production in freshwater river sediments. *Environ. Sci. Technol.* 46, 2684–2691.
- Yu, R.-Q., Reinfelder, J.R., Hines, M.E., Barkay, T., 2018. Syntrophic pathways for microbial mercury methylation. *ISME J.* 12, 1826–1835.